



Effect of Atmospheric Pressure Plasma Treatment on the Lap-Shear Strength of Adhesive-Bonded Sheet Molding Compound Joints

Shuang Wang¹ · Junying Min^{1,2} · Jianping Lin^{1,2} · Chengcheng Sun¹ · Shanglu Yang³

Received: 6 February 2018 / Accepted: 27 July 2018 / Published online: 23 August 2018
© The Author(s) 2018

Abstract

Atmospheric pressure plasma treatment (APPT) technology was used herein to treat sheet molding compound (SMC) substrates to increase the lap-shear strength of adhesive-bonded SMC joints. Further, the mechanisms behind the lap-shear strength improvements in APPT-treated adhesive-bonded SMC joints were explored. A maximum lap-shear strength about three times that of the as-received SMC joints was achieved when the APPT distance was set to 20 mm. The surface roughness, which exhibited little benefit to the lap-shear strength, was determined to not be the primary reason for the increase in lap-shear strength. Specifically, X-ray photoelectron spectra revealed that an increased amount of O-containing groups (i.e., C–O–H, C–O–C, H–O–C=O or R–O–C=O) following APPT contributed to the improved lap-shear strength. In addition, the surface free energy increased significantly after APPT, which improved the lap-shear strength of the adhesive-bonded SMC joints. Compared to the change of surface morphology, the changes in both the surface chemical property and surface free energy played larger roles in increasing the lap-shear strength of APPT-treated SMC joints.

Keywords Plasma treatment · Sheet molding compound · Lap-shear strength · Chemical properties · Surface free energies

1 Introduction

Sheet molding compounds (SMCs) have gained extensive use in the area of new-energy vehicles to realize the light-weight requirements thereof [1, 2]. However, a method whereby to joint the SMC substrates to ensure adequate automotive safety becomes important as the number of joining demands increases [3]. Adhesive bonding has the advantages of excellent mechanical properties, uniform stress distribution and low damage to the SMC substrates compared with the conventional joining techniques of welding and bolted connections [4]. Therefore, adhesive bonding has emerged as one

of the most effective joining methods for SMC. However, the SMC joints are not widely used as-received because of their poor lap-shear strength caused by the mold release agent used during demolding [5]. To achieve a greater and more durable lap-shear strength, the surface of the SMC substrates must therefore be cleaned and activated before joint fabrication [6]. Previous studies have reported adhesion improvements after wet chemical cleaning or mechanical abrasion [7]. Recently, the atmosphere pressure plasma treatment (APPT) technology has become more important in surface modifications of composites owing to its advantages of environmental protection and high efficiency [8, 9]. Furthermore, as a functional technique, it affects only the substrate surface and changes the surface properties.

The APPT is widely applied as a polymer pre-treatment in practical situations [10, 11]. It is worth noting that the APPT has drawn the attention of both industry and academy in recent years because of its ease of operation in industrial production and its selective treatment of substrates [12]. In a previous study, Noeske et al. [10] have found that the joints of polyethylene, polypropylene, polyvinylidene fluoride, polymers polyethyleneterephthalate and polyamide-6 following plasma treatment exhibited the fracture modes of substrate failure and cohesive failure after tensile test-

✉ Junying Min
Junying.Min@tongji.edu.cn

✉ Jianping Lin
jplin58@tongji.edu.cn

¹ School of Mechanical Engineering, Tongji University, Shanghai 201804, China

² Key Lab of Vehicle Aerodynamics and Vehicle Thermal Management Systems of Shanghai, Tongji University, Shanghai 201804, China

³ Shanghai Institute of Optics and Fine Mechanics, Shanghai 201800, China

ing, while the as-received joints exhibited adhesive failure between the polymer and adhesive. Gonzalez and Hicks [13] have investigated the surface modifications of polymers after remote APPT, while Zaldivar et al. [14] have used APPT to improve the strength of composites. Additionally, Yun et al. [15] have studied how the APPT affects polyimide/novolac epoxy resin joints using various gas types and aging temperatures. However, few studies exist on the mechanism of activating SMC substrates by APPT. The surface of substrates can be damaged or melted by high gas temperatures, induced by the heat sensitivity of the fiber-reinforced polymer. The optimal parameters for the application of this relatively new plasma treatment need to be studied in detail. Therefore, it is essential to explore the effects of APPT on the surface properties and adhesion performances of SMC substrates.

In this study, APPT was used to clean the surface and activate the SMC substrates. Quasi-static lap-shear testing was used to estimate the effect that APPT had on the lap-shear strength. Scanning electron microscopy (SEM) and roughness measurements were used to estimate the morphology modifications following APPT, while X-ray photoelectron spectroscopy (XPS) was used to characterize the chemical properties of the plasma-treated and as-received SMC substrates. Finally, the effect of APPT on the wettability of the SMC substrates was evaluated in the respect of contact angle and surface free energy (SFE).

2 Experimental Details

2.1 Materials

The SMC used herein was fabricated from carbon fiber and vinyl ester resin and was strengthened by a fairly high proportion of short carbon fibers. The versatile epoxy backbone and the modifiers included in the resin system increased the toughness of the SMC. A mold release agent was used in the molding process. The SMC plates 3 mm thick were cut into substrates $100 \times 25 \text{ mm}^2$ in area. A two-component room-temperature-cured epoxy adhesive (Scotch-Weld DP460, 3 M) was used to joint the APPT-treated and as-received SMC substrates. The mechanical properties of the SMC used herein and the fully cured structural adhesive at room temperature are listed in Tables 1 and 2, respectively.

2.2 Plasma Treatment

The APPT apparatus illustrated in Fig. 1a was employed to treat the SMC substrates. In the plasma treatment process, a plasma jet flowing from a circular nozzle was sprayed over the SMC substrate, whose path is illustrated in Fig. 1b. The width of the plasma jet was set at 4 mm, and the treated

Table 1 Mechanical properties of the sheet molding compound used herein

Material	Elastic modulus (GPa)	Tensile strength (MPa)	Density (g/cm ³)
SMC	19.7	108	1.3

Table 2 Mechanical properties of the fully cured 3M DP460 adhesive [16]

Adhesive	Elastic modulus (GPa)	Tensile strength (MPa)	Shear strength (MPa)	Poisson ratio
3M DP460	2.7	37	32	4

area of SMC substrates ($14 \times 25 \text{ mm}^2$) was chosen to be slightly wider than the bonding area ($12.5 \times 25 \text{ mm}^2$). The gas flow pressure was set to 0.25 MPa for all substrates, and the atmospheric speed close to the exit of the circular nozzle was 7.2 m/s. Further, an operating discharge voltage of 8 kV and a discharge frequency of 12 kHz were used. To achieve a continuous treatment across the substrate area, the SMC substrates were placed on an automated moving platform that had a lateral speed of 10 mm/s. According to previous studies [17–19], the lap-shear strength of the adhesive-bonded joints is related to several factors of the APPT process such as the distance between the substrate and APPT apparatus nozzle, the working gas, and the duration of APPT exposure. In this work, the distance between the APPT apparatus nozzle and the substrate was varied to explore its effect on the lap-shear strength of the adhesive-bonded SMC joints. Vertical distances between the nozzle and the SMC substrates of 25, 20, 15, and 10 mm were used, and a photograph of the plasma jet operating with a treatment distance of 10 mm is given in Fig. 2.

2.3 Adhesive-Bonded Joint Fabrication

Figure 3 schematically illustrates the configurations and detailed dimensions of lap-shear adhesive-bonded SMC joints. The fabrication process of the adhesive-bonded SMC joints comprised the following procedure: (1) The 3 M DP460 adhesive was applied with a glue gun onto the bonding region of the substrate. (2) Glass drops with the diameter of 0.25 mm were sprayed into the adhesive to set the thickness of the adhesive layer during the next process step. (3) A fixture was used to provide pressure on the surfaces of the two joined SMC substrates. (4) Any adhesive that was pushed outside of the bonding region was removed. (5) The joints were cured for 24 h at 25 °C, as recommended by the adhesive supplier.

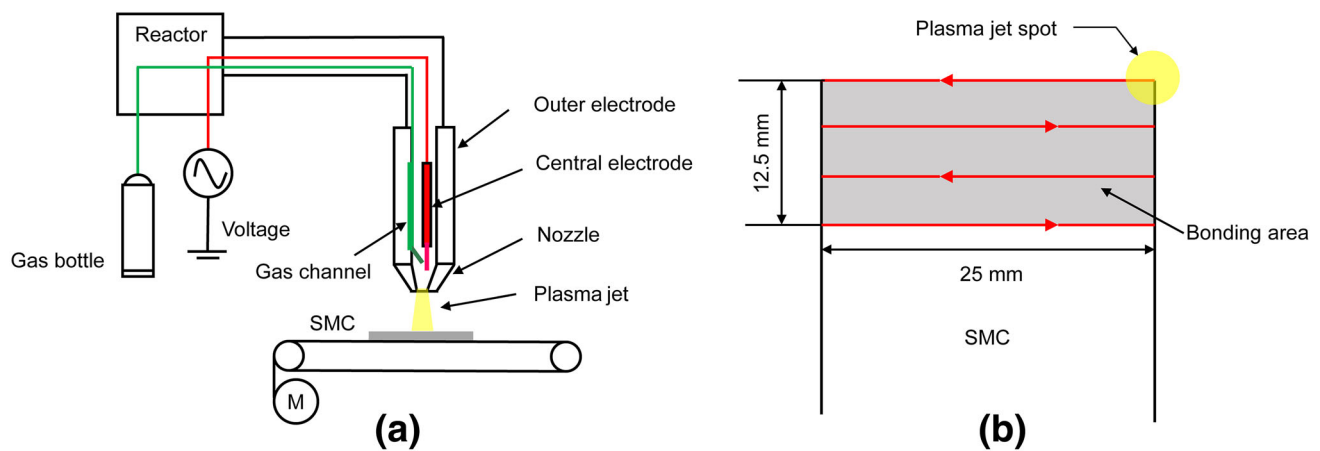


Fig. 1 **a** Diagrammatic illustration of APPT apparatus and **b** illustration of the plasma jet path on the SMC substrate

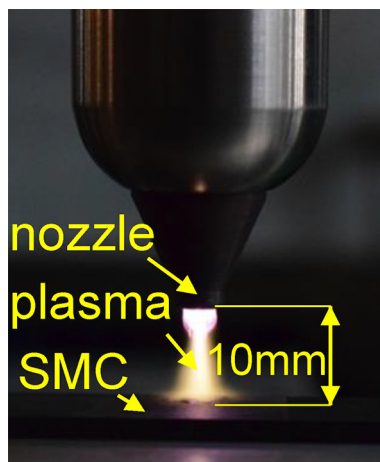


Fig. 2 Photograph of a plasma jet operating at a nozzle-substrate distance of 10 mm

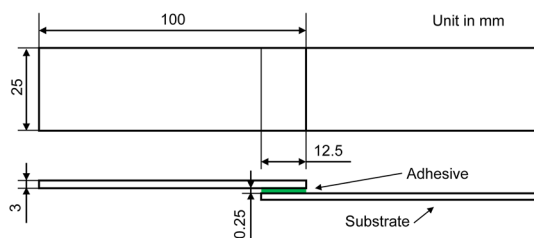


Fig. 3 Configuration and detailed dimensions of the lap-shear adhesive-bonded joint

2.4 Quasi-Static Lap-Shear Tensile Test

Using the ASTM D1002-2001 test method standard [20], quasi-static lap-shear tensile tests of the adhesive-bonded SMC joints were carried out to determine the lap-shear strength in a universal testing machine (MTS Systems Corp.). To mitigate bending during the lap-shear tensile test of the adhesive-bonded SMC joints, two plates 3.0 mm thick were

applied, which ensured that the tensile direction was roughly parallel to the SMC joint. To obtain the peak loads of the lap-shear joints, the crosshead speed was set at 2 mm/min until fracture. The lap-shear strength was acquired as an average value of five measurements obtained with the same conditions. Finally, analysis of the fracture surface was performed to estimate the fracture modes of the adhesive-bonded joints.

2.5 Characterization of Surface Morphologies

The influence that APPT has on the SMC substrate surface morphology was studied with SEM, while the surface roughness of the SMC substrates was measured by a 3D optical profiler. In this way, accurate measurements were obtained of the modifications induced on the substrate surface morphology by APPT.

2.6 Surface Chemistry Analysis

The surface chemistry state of the APPT-treated and as-received SMC substrates was characterized by XPS (Escalab 250Xi, Thermo Scientific) whose X-ray source had a spot size of 500 μm . In the XPS spectra, the peak at 284.6 eV was referenced as C 1 s. In addition, a complete analysis of the different peaks was conducted using a Lorentzian-Gaussian peak shape.

2.7 Contact Angle Measurement and SFE

Surface wettability, which is an essential factor for improving adhesion, is commonly evaluated using contact angle values and the SFE [21]. Here, the contact angles on the

Table 3 Surface tension data of the testing liquids [22]

Liquid	Surface tension data (mJ/m ²)		
	γ	γ^d	γ^p
Distilled water	72.8	21.8	51.0
Diiodomethane	50.8	50.8	0
Ethylene glycol	48.0	29.0	19.0

SMC substrate surfaces were measured by the contact angle measurement system (OCA-20, Dataphysics) previously described in Ref. [22]. Table 3 lists the room-temperature surface tension data of the three contact angle testing liquids (i.e., distilled water, diiodomethane, and ethylene glycol), where the test liquid drop volume was 2 μ L. The contact angle was calculated by sessile drop technology, where each average contact angle was calculated based on five identical measurements.

The SFE of the SMC substrates was calculated using Young's equation (refer to Eq. (1)), which represents the relation between the contact angle θ and the SFE [23]. The interfacial energy between the solid and the liquid γ_{SL} can be expressed as

$$\gamma_S = \gamma_{SL} + \gamma_L \cos \theta, \quad (1)$$

where γ_S and γ_L are the SFE values of the solid and liquid, respectively [24].

Owens and Wendt [25] have proposed a geometrical way of connecting the dispersion and polar interactions in accordance with the ideas of Fowkes [26]. Following their proposal, the estimation for γ_{SL} was expressed as

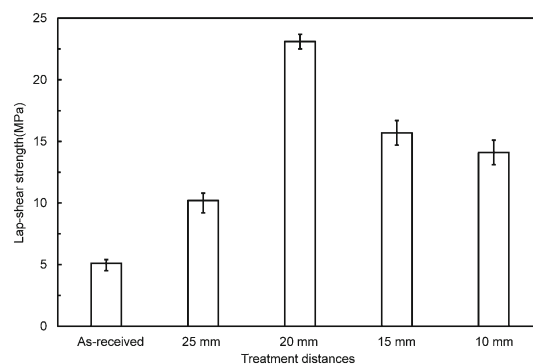
$$\gamma_{SL} = \gamma_S + \gamma_L - 2\sqrt{\gamma_S^d \gamma_L^d} - 2\sqrt{\gamma_S^p \gamma_L^p}, \quad (2)$$

where γ_S^d and γ_L^d are the dispersion components of SFE values of the solid and liquid, respectively, where γ_S^p and γ_L^p are the polar component of SFE values of the solid and liquid, respectively.

Substituting Eq. (1) into Eq. (2) yields

$$\gamma_L(1 + \cos \theta) = 2\sqrt{\gamma_S^d \gamma_L^d} + 2\sqrt{\gamma_S^p \gamma_L^p}. \quad (3)$$

To acquire the γ_S^d and γ_S^p values of the solid, we need to measure the contact angles of more than two liquid types whose surface tension components can be acquired. Herein, three typical measuring liquid types were involved to determine the γ_S^d and γ_S^p of the SMC substrates.

**Fig. 4** Lap-shear strengths of SMC joints in as-received condition and after APPT at various distances

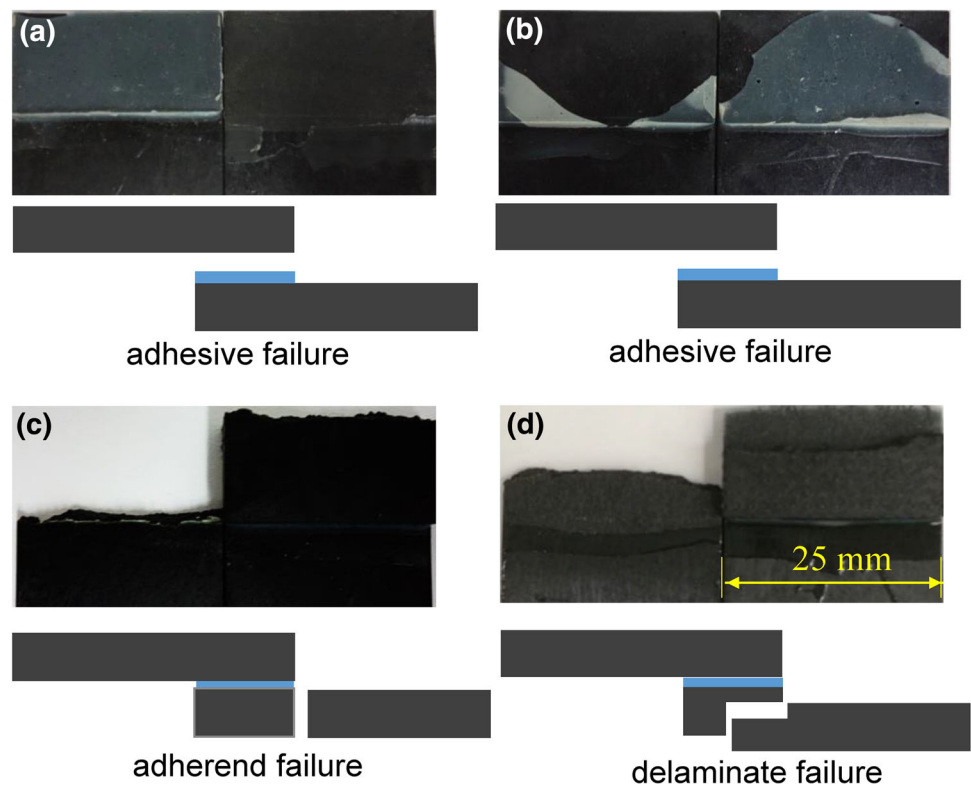
3 Results and Discussion

3.1 Lap-Shear Strength of Adhesive-Bonded SMC Joints

Figure 4 shows the lap-shear strengths of the adhesive-bonded SMC joints as-received and after APPT at various distances. The lap-shear strength of the as-received SMC joint was 5.1 MPa and increased to 10.2 MPa after APPT at a distance of 25 mm. When the APPT distance was 20 mm, the lap-shear strength reached its maximum of 23.1 MPa. Further, as the APPT distance decreased to 15 and 10 mm, the lap-shear strengths decreased to 15.7 and 14.1 MPa, respectively.

The fracture mode of the adhesive-bonded joint is another indicator that can be used to evaluate the adhesive bonding performance. The fracture modes of various SMC joints are shown in Fig. 5. The fracture mode of the as-received SMC joint in Fig. 5a was adhesive failure, which indicated that the interface strength between the adhesive and the as-received SMC substrates was less than the shear strength of the 3 M DP460 adhesive. With APPT at a distance of 25 mm, the fracture mode was also adhesive failure, as suggested by Fig. 5b. With APPT at a distance of 20 mm, the fracture mode of the joints was adherend failure (Fig. 5c), which presented with a neat fracture at the bonding edge. In addition, the lap-shear strength reached 23.1 MPa. We note the lap-shear strength herein was always lower than 25.9 MPa. This is owing to the fact that the SMC substrates will fracture if the tensile force reaches 8.1 kN ($108 \text{ MPa} \times 25 \text{ mm} \times 3 \text{ mm} = 8.1 \text{ kN}$) according to the tensile strength of SMC in Table 1, and the fact that for adhesive-bonded joints the lap-shear strength is 25.9 MPa ($8.1 \text{ kN}/(12.5 \text{ mm} \times 25 \text{ mm}) = 25.9 \text{ MPa}$) when the tension reaches to 8.1 kN. In addition, a bending moment exists at the junction of the joints. Therefore, the lap-shear strength value was always lower than 25.9 MPa. At the same time, the interface strength between the SMC substrates and adhesive was higher than 23.1 MPa as evidenced by the lack

Fig. 5 Fracture modes of **a** as-received SMC joints and **b–d** SMC joints undergoing APPT at distances of **b** 25, **c** 20 and **d** 15 and 10 mm



of adhesive failure. When the APPT distance was either 15 or 10 mm, the fracture mode was a thin delamination fracture, as shown in Fig. 5d. This is owing to the fact that at APPT distances of 15 and 10 mm the substrate temperature will increase to levels that can damage the SMC substrates and thus induce a delamination fracture. Furthermore, this indicates that the interface strengths produced at APPT distances of 15 and 10 mm are also greater than the strength between the carbon fiber and vinyl ester resin. Because the fracture modes in samples with treatment distances of 20, 15 and 10 mm were either adherend or delamination failure, the specific interface strength values between the adhesive and APPT-treated SMC substrates could not be measured. Nevertheless, according to Figs. 4 and 5, the interface strength between the adhesive and SMC substrates was improved after APPT. Additionally, the interface strengths at APPT distances of 20, 15 and 10 mm were higher than that with an APPT distance of 25 mm.

This relationship between the fracture mode and interface strength indicates that the interface strength between the SMC substrates and adhesive was enhanced by the APPT. To understand the reasons underlying the interface strength increase following APPT, further analyses were performed that focused on as-received SMC substrates and APPT-treated SMC substrates at treatment distances of 25 and 20 mm. The effect of APPT on the surface morphologies, chemical properties and SFE of SMC substrates will be explored in detail.

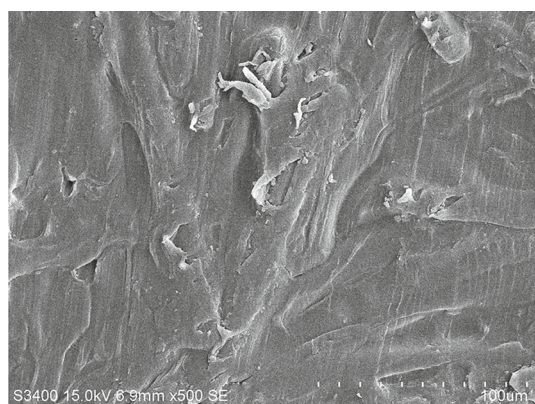
3.2 Surface Morphologies of Plasma-Treated SMC Substrates

Figure 6 presents the surface morphologies of APPT-treated and as-received SMC substrates. In Fig. 6a, we observe that the as-received SMC substrate surface morphologies are relatively out-of-flatness and that some material exists above the SMC substrates, which is most likely the release agent applied for the molding process. Much more uniform surface morphologies after APPT are observed in Fig. 6b, c, which indicates that the plasma jet removed SMC substrate surface material (e.g., the release agent and possibly somewhat of the resin).

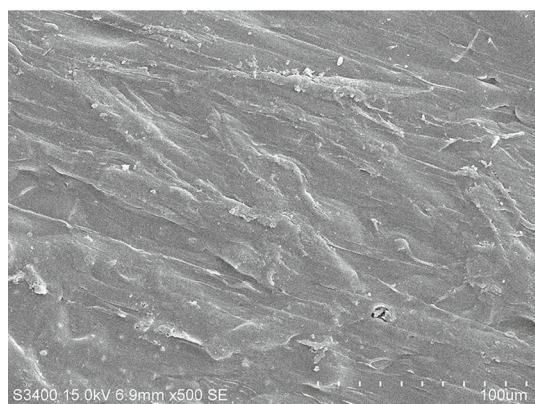
Roughness testing was used to estimate the surface morphology modification of SMC substrates induced by APPT. Figure 7 exhibits the surface roughness (R_a) values of APPT-treated and as-received SMC substrates, where it can be found the APPT treatment at the distances of 25 and 20 mm did not have an obvious effect on the surface roughness. This result is consistent with the SEM micrographs in Fig. 6.

3.3 Chemical Properties of Plasma-Treated SMC Substrates

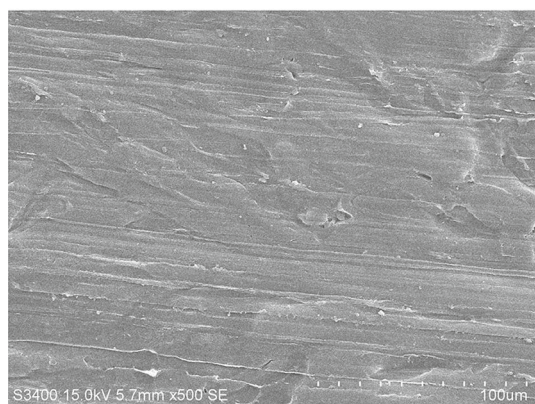
Typical XPS survey spectra for the APPT-treated (20 and 25 mm distances) and as-received SMC substrates are given in Fig. 8, wherein obvious and intense peaks emerging in the spectra of the three samples demonstrate the existence of C



(a) As-received



(b) 25 mm



(c) 20 mm

Fig. 6 SEM images of **a** as-received SMC substrates and **b, c** SMC substrates undergoing APPT at distances of **b** 25 and **c** 20 mm

1 s, O 1 s, N 1 s and Si 2p. The quantified XPS results of APPT-treated SMC substrates are presented in Table 4, where the amount of silicon is observed to decrease after APPT while the amount of nitrogen increased gradually with decreasing distance between the APPT nozzle and SMC substrate.

Mold release agents are widely applied in SMC substrate fabrication where silicone elastomer-polydimethylsiloxane, comprising silicon–oxygen–silicon as chain and side-

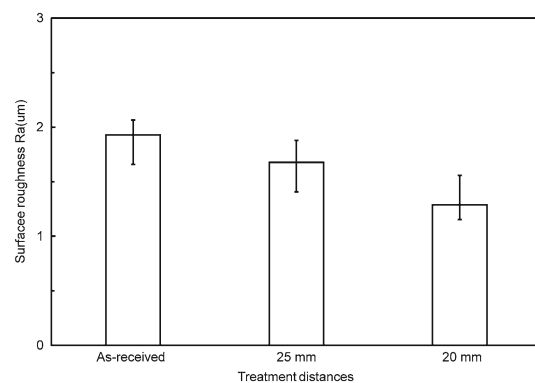


Fig. 7 Surface roughness values of SMC substrates

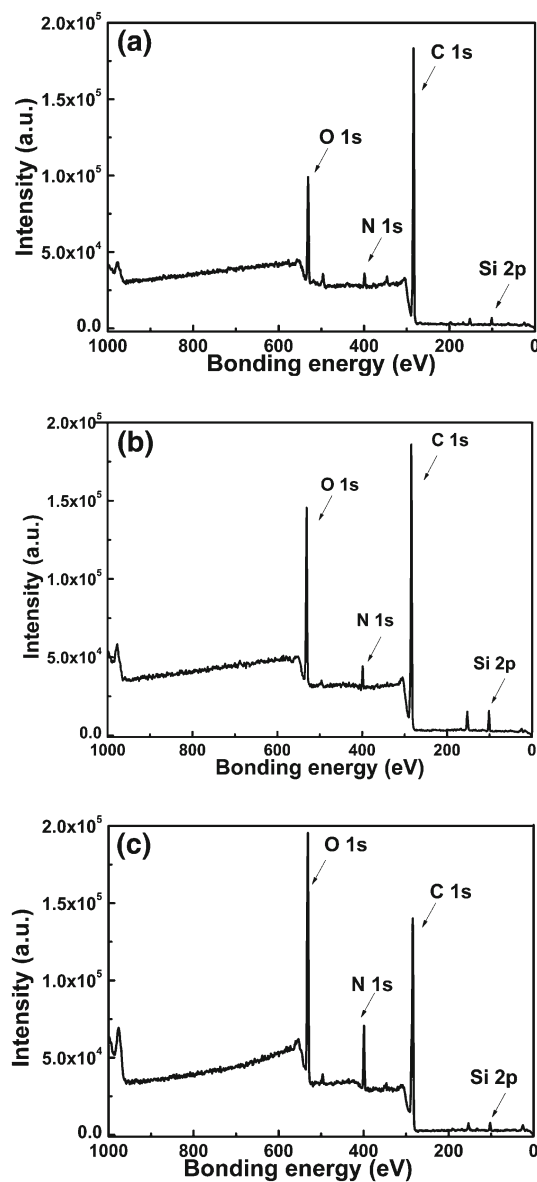


Fig. 8 XPS spectra of various SMC substrates: **a** as-received SMC and **b, c** SMC substrates undergoing APPT at distances of **b** 25 and **c** 20 mm

Table 4 The quantified XPS results of the chemical composition of as-received and APPT-treated SMC substrates

	O	C	N	Si
As-received	10.3	81.8	3.9	3.2
25 mm plasma	14.5	78.8	4.5	1.9
20 mm plasma	21.3	68.1	8.9	1.1

chained carbon atoms, is the main component of the mold release agent. In the results herein, the amount of silicon decreased following APPT, which suggested that the mold release agent was gradually removed by the APPT. The increasing nitrogen amount was owing to the fact that nitrogen compounds present in the air entered the surface of resin when plasma treatment was applied [27].

Further, the amount of oxygen increased and the amount of carbon decreased significantly after plasma treatment. To further probe the detailed chemical states of carbon present in the samples, narrow-scan spectra were obtained and peak differentiation analyses were conducted. The XPS C 1 s binding energy spectra are shown in Fig. 9, and the functional group distributions on the surface of the SMC substrates are given in Table 5. The carbon signal is commonly used to calibrate the energy of the other existing signals in the XPS spectrum, so it is a trustworthy signal from which we can derive relative amounts. Here, the C 1 s peak was deconvoluted and found to divide into three distinct peaks. The peak at 284.6 eV corresponds to C–C or C–H bonds [28, 29], while the higher oxidation states of carbon located at 286.7 eV correspond to C–O–H or C–O–C functional groups [28, 29]. Finally, the peak at 288.5 eV is attributed to H–O–C=O or R–O–C=O groups [30, 31]. The low oxidation states of carbon (i.e., peak at 284.6 eV) experienced a decreased signal intensity after APPT. The amounts of the three types of chemical bonds and the O/C ratio can be obtained from the deconvoluted C 1 s peak, and Table 5 clearly shows that the APPT increased the O/C ratio. When the APPT distance was 20 mm the O/C ratio was at a maximum, which is consistent with the O 1 s spectra results shown in Table 4. In addition, it can be seen that the amount of groups containing the C element had a dramatic decline and the amount of O-containing groups (C–O–H, C–O–C, H–O–C=O, R–O–C=O) strongly increased as the treatment distance decreased to 20 mm.

3.4 SFE of APPT-Treated SMC Substrates

The contact angles (illustrated in Fig. 10) of three kinds of liquids on the SMC substrates are listed in Table 6. After APPT, the contact angles of distilled water on SMC substrates decreased obviously, and thus APPT contributes to the wettability of SMC substrates. The SFE of the SMC sub-

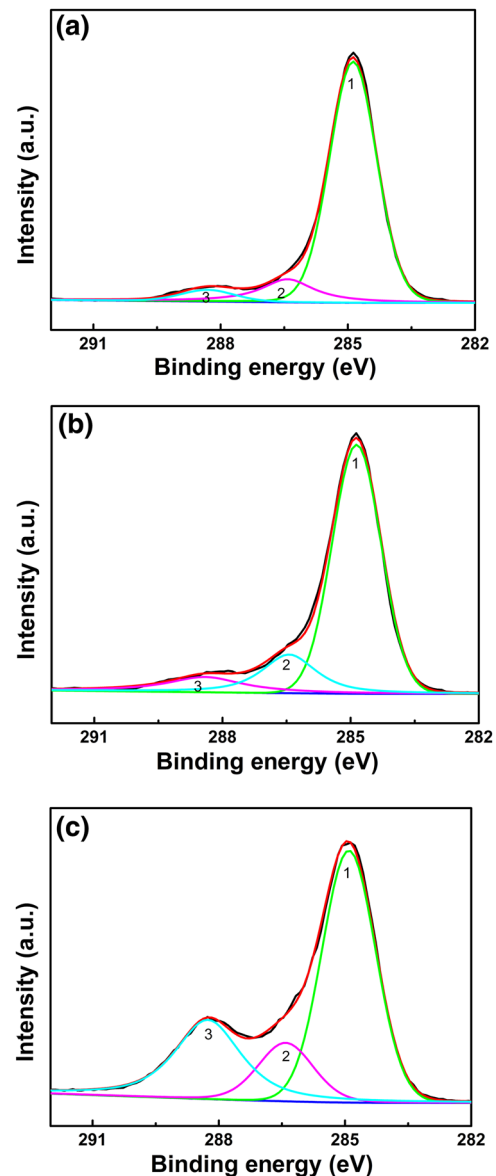


Fig. 9 Carbon 1 s XPS spectra on the surface of **a** as-received and **b, c** APPT-treated SMC substrates treated at distances of **b** 25 and **c** 20 mm. The peaks are labeled to correspond to C–C/C–H (1), C–O–H/C–O–C (2), and COOH/COOR (3)

strates was estimated based on the method introduced by Owens and Wendt [25] and by Fowkes [26]. It was found that the SFE, which consisted of polar and dispersion components, increased significantly after APPT, as presented in Fig. 11. The SFE of the as-received SMC substrates mainly possessed a dispersion component of about 27.18 mJ/mm², while the polar component was only 3.26 mJ/mm². The dispersion component exhibited almost no change after plasma treatment while, interestingly, the polar component increased remarkably to 12.04 and 36.20 mJ/mm² as the treatment distances reached to 25 and 20 mm, respectively.

Table 5 Relative peak areas (%) obtained via C 1 s peak deconvolution and the three chemical bond types on the surface of as-received and APPT-treated SMC substrates

	Peak	Binding energy (eV)	Assignment	Relative peaks area (%)		
				As-received	25 mm plasma	20 mm plasma
C 1 s	1	284.6	C–C/C–H	80.7	70.3	56.7
	2	286.7	C–O–H/C–O–C	12.6	20.9	19.7
	3	288.5	COOH/COOR	6.7	8.8	23.6
O/C ratio				12.6	18.4	31.3

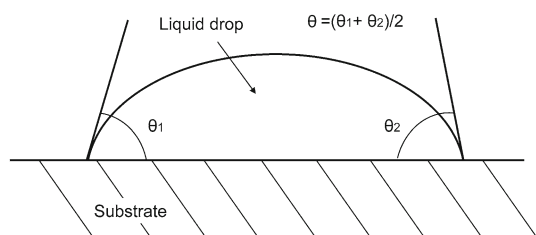


Fig. 10 Diagrammatic illustration of the contact angle parameters

3.5 Discussion

Based on the above results, the lap-shear strength of adhesive-bonded SMC joints was found to be remarkably enhanced by APPT. When the treatment distance was 20 mm, the maximum lap-shear strength was obtained, which was about three times more than the lap-shear strength of the as-received SMC joint. This increase in lap-shear strength was related with the enhanced amount of O-containing groups (C–O–H, C–O–C, H–O–C=O or R–O–C=O), as shown in Fig. 8 and Table 5. Ni et al. [32] have found that, following APPT, the amount of ester groups (R–O–C=O) on the substrate surface decreased, whereupon more carboxyl groups (H–O–C=O) and hydroxyl groups (C–O–H) appeared. This offers an explanation for the increasing amount of carboxyl groups (H–O–C=O) and hydroxyl groups (C–O–H) following APPT. Blank et al. [33] have confirmed that chemical reactions can exist between epoxide groups and carboxyl or hydroxyl groups, which can operate as a crosslinking mechanism, as shown in Fig. 12. The possible reactions that may appear between the residual epoxide groups of the adhesive and the carboxyl groups (H–O–C=O) and hydroxyl groups (C–O–H) are exhibited in Fig. 13. These reactions suggest that APPT can cause the chemical groups of vinyl ester resin to become more active, which facilitates the combination of

Table 6 Effect of APPT on contact angles of three kinds of testing liquids

Treatment distance	Distilled water		Ethylene glycol		Diiodomethane	
	CA (°)	SD	CA (°)	SD	CA (°)	SD
As-received	100.8	0.90	72.5	1.12	62.4	0.88
25 mm	73.4	1.24	40.5	1.71	60.5	0.98
20 mm	53.1	1.22	20.1	1.16	59.9	1.02

CA contact angle, SD standard deviation

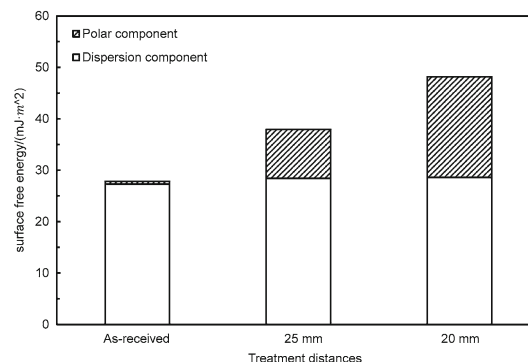


Fig. 11 Calculated surface free energies of SMC substrates

resin and adhesive. Finally, as reported by Zaldivar et al. [34], an increased amount of carboxyl groups can improve the lap-shear strength.

The SFE was found to increase significantly after APPT, and two reasons were posited to explain this phenomenon. First, the APPT increased the amount of oxygen, which facilitated the existence of polar molecules. Zaldivar et al. [34] have also concluded that wetting characteristics are influenced positively by the amount of oxygen. Second, the APPT removed the inert mold release agent present on the SMC substrates, where the former possesses a low surface tension.

Additionally, to clearly compare the relationship between the lap-shear strength and the surface roughness, the lap-shear strength and roughness of SMC substrates treated with APPT at various distances are shown in Fig. 14. Similar surface roughnesses are observed on the APPT-treated and as-received SMC substrates, but the lap-shear strengths varied remarkably. It may be concluded that the surface morphology modifications were not responsible for the variation of the lap-shear strength. Specifically, the surface roughness contributed little benefit to the lap-shear strength and was not

Fig. 12 The chemical reactions of **a** an epoxide group and a carboxyl group and **b** an epoxide group and a hydroxyl group [31]

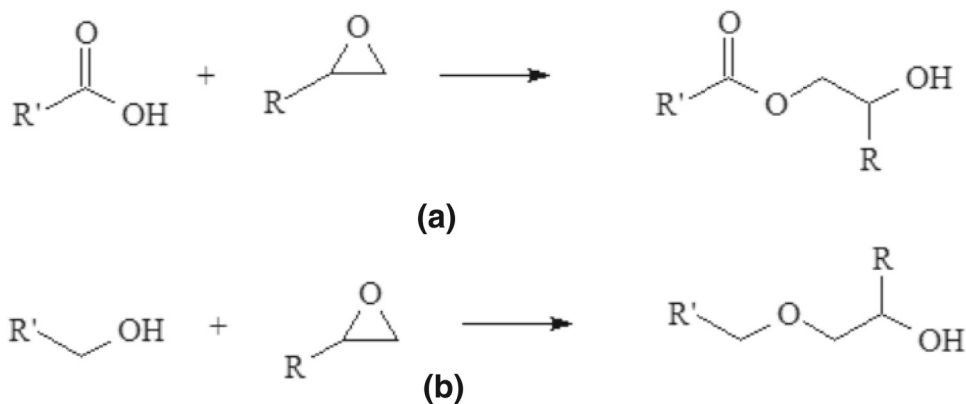


Fig. 13 Possible chemical combination between the residual epoxide groups of the adhesive and the carboxyl or hydroxyl groups

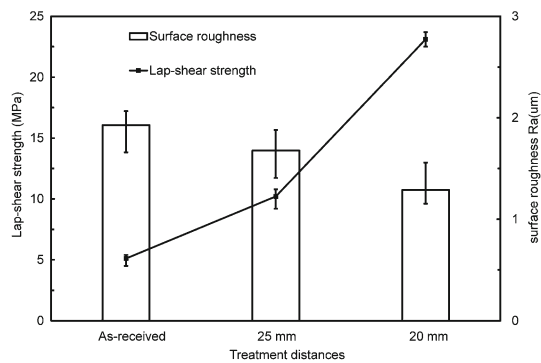
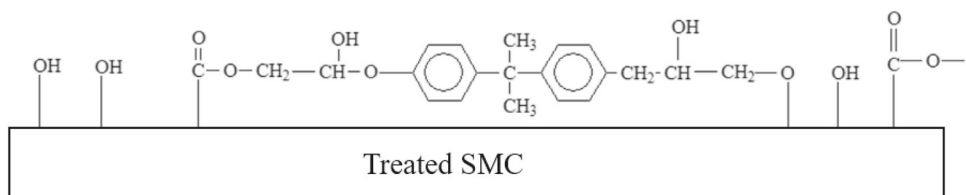


Fig. 14 Lap-shear strengths and roughness of as-received and APPT-treated SMC substrates treated at various distances

the primary reason for the increase in the lap-shear strength of APPT-treated SMC joints. On the contrary, the change of chemical properties had an important effect on the increase in the lap-shear strength, which agrees with the viewpoint of Zaldivar et al. [35] and Schafer et al. [36]. In particular, the hydroxyl and carboxyl groups increased significantly after APPT and may be the primary reason for the improvement in the lap-shear strengths of APPT-treated SMC joints.

4 Conclusions

In this study, the effects of APPT on the adhesive bonding performance of SMC joints were explored. Some conclusions can be drawn, as follows:

1. The maximum lap-shear strength of the APPT-treated adhesive-bonded joints (about three times more than that of the as-received joints) was achieved when the APPT distance was set to 20 mm.

2. Surface roughness exhibited little benefit to the lap-shear strength of the adhesive-bonded SMC joints, indicating that the change of surface roughness does not fully account for the increased lap-shear strengths of adhesive-bonded SMC joints. The chemical property and SFE, however, play important roles in improving the lap-shear strength of the adhesive-bonded SMC joint.
3. The APPT can increase the amount of O-containing groups (C–O–H, C–O–C, H–O–C=O or R–O–C=O) and the O/C ratio existing on the SMC substrates. In particular, increased amounts of hydroxyl and carboxyl groups after APPT remarkably improve the lap-shear strength of adhesive-bonded SMC joints.
4. The SFE increased significantly after APPT owing to the removal of the mold release agent present on the as-received SMC substrate surface and to the increased amount of oxygen.

Acknowledgements This work was supported by the National Natural Science Foundation of China (Grant No. 51575397).

Open Access This article is distributed under the terms of the Creative Commons Attribution 4.0 International License (<http://creativecommons.org/licenses/by/4.0/>), which permits unrestricted use, distribution, and reproduction in any medium, provided you give appropriate credit to the original author(s) and the source, provide a link to the Creative Commons license, and indicate if changes were made.

References

1. McConnell, V.P.: New recipes for SMC innovation. *Reinf. Plast.* **52**(8), 34–39 (2008)

2. Min, J., Li, Y., Li, J., et al.: Friction stir blind riveting of carbon fiber-reinforced polymer composite and aluminum alloy sheets. *Int. J. Adv. Manuf. Tech.* **76**(5–8), 1403–1410 (2015)
3. Adams, R.D.: *Adhesive Bonding: Science, Technology and Applications*. CRC Press, Boca Raton (2005)
4. Da Silva, L.F.M., Ochsner, A., Adams, R.D.: *Handbook of Adhesion Technology*. Springer, Heidelberg (2011)
5. Kim, J.K., Lee, D.G.: Adhesion characteristics of plasma-surface-treated carbon fiber-epoxy composite with respect to release films used during demolding. *J. Adhes. Sci. Technol.* **18**(4), 473–494 (2004)
6. Belmonte, G.K., Charles, G., Strumia, M.C., et al.: Permanent hydrophilic modification of polypropylene and poly (vinyl alcohol) films by vacuum ultraviolet radiation. *Appl. Surf. Sci.* **382**, 93–100 (2016)
7. Wells, J.C., Thompson, B.T., Dillard, J.G.: The effect of surface preparation and exposure environment on the bond failure processes in adhesively bonded sheet molded composite (SMC). *J. Adhes.* **48**(1–4), 217–234 (1995)
8. Akram, M., Jansen, K.M.B., Ernst, L.J., et al.: Atmospheric plasma modification of polyimide sheet for joining to titanium with high temperature adhesive. *Int. J. Adhes. Adhes.* **65**, 63–69 (2016)
9. Hegemann, D., Brunner, H., Oehr, C.: Plasma treatment of polymers for surface and adhesion improvement. *Nucl. Instrum. Methods Phys. Res. Sect. B* **208**, 281–286 (2003)
10. Noeske, M., Degenhardt, J., Strudthoff, S., et al.: Plasma jet treatment of five polymers at atmospheric pressure: surface modifications and the relevance for adhesion. *Int. J. Adhes. Adhes.* **24**(2), 171–177 (2004)
11. Shenton, M.J., Stevens, G.C.: Surface modification of polymer surfaces: atmospheric plasma versus vacuum plasma treatments. *J. Phys. D Appl. Phys.* **34**(18), 2761–2768 (2001)
12. Merche, D., Vandencastele, N., Reniers, F.: Atmospheric plasmas for thin film deposition: A critical review. *Thin Solid Films* **520**(13), 4219–4236 (2012)
13. Gonzalez, E., Hicks, R.F.: Surface analysis of polymers treated by remote atmospheric pressure plasma. *Langmuir* **26**(5), 3710–3719 (2009)
14. Zaldivar, R.J., Steckel, G.L., Morgan, B.A., et al.: Bonding optimization on composite surfaces using atmospheric plasma treatment. *J. Adhes. Sci. Technol.* **26**(1–3), 381–401 (2012)
15. Yun, H.K., Cho, K., Kim, J.K., et al.: Effects of plasma treatment of polyimide on the adhesion strength of epoxy resin/polyimide joints. *J. Adhes. Sci. Technol.* **11**(1), 95–104 (1977)
16. Sun, C., Min, J., Lin, J., et al.: The effect of laser ablation treatment on the chemistry, morphology and bonding strength of CFRP joints. *Int. J. Adhes. Adhes.* **84**, 325–334 (2018)
17. Laroussi, M., Akan, T.: Arc-free atmospheric pressure cold plasma jets: a review. *Plasma Process. Polym.* **4**(9), 777–788 (2007)
18. Teixeira, H.S., Coelho, P.G., Duarte, S., et al.: Influence of atmospheric pressure plasma treatment on mechanical properties of enamel and sealant bond strength. *J. Biomed. Mater. Res. B Appl. Biomater.* **103**(5), 1082–1091 (2015)
19. Zaldivar, R.J., Kim, H.I., Steckel, G.L., et al.: Effect of processing parameter changes on the adhesion of plasma-treated carbon fiber reinforced epoxy composites. *J. Compos. Mater.* **44**(12), 1435–1453 (2010)
20. ASTM D1002-2001. Standard Test Method for Apparent Shear Strength of Single-Lap-Joint Adhesively Bonded Metal Specimens by Tension Loading (Metal-to-Metal). American Society for Testing Materials
21. Baldan, A.: Adhesion phenomena in bonded joints. *Int. J. Adhes. Adhes.* **38**, 95–116 (2012)
22. Wang, X., Lin, J., Min, J., et al.: Effect of atmospheric pressure plasma treatment on strength of adhesive-bonded aluminum AA5052. *J. Adhes.* **2018**, 1–22 (2017)
23. Young, T.: III. An essay on the cohesion of fluids. *Philos. Trans. R. Soc. Lond.* **95**, 65–87 (1805)
24. Kim, J.K.: Characteristics of plasma surface treated composite adhesive joints at high environmental temperature. *Compos. Struct.* **57**(1–4), 37–46 (2002)
25. Owens, D.K., Wendt, R.C.: Estimation of the surface free energy of polymers. *J. Appl. Polym. Sci.* **13**(8), 1741–1747 (1969)
26. Fowkes, F.M.: Attractive forces at interfaces. *Ind. Eng. Chem.* **56**(12), 40–52 (1964)
27. Bubert, H., Ai, X., Haiber, S., et al.: Basic analytical investigation of plasma-chemically modified carbon fibers. *Spectrochim. Acta Part B* **57**(10), 1601–1610 (2002)
28. Li, H., Liang, H., He, F., et al.: Air dielectric barrier discharges plasma surface treatment of three-dimensional braided carbon fiber reinforced epoxy composites. *Surf. Coat. Technol.* **203**(10), 1317–1321 (2009)
29. Briggs, D., Seah, M.P.: *Practical Surface Analysis: Auger and X-ray Photoelectron Spectroscopy*, vol. 1. Wiley, Chichester (1990)
30. Xie, J., Xin, D., Cao, H., et al.: Improving carbon fiber adhesion to polyimide with atmospheric pressure plasma treatment. *Surf. Coat. Technol.* **206**(2), 191–201 (2011)
31. Chen, S., Wang, S., Wang, Y., et al.: Surface modification of epoxy resin using He/CF₄ atmospheric pressure plasma jet for flashover withstanding characteristics improvement in vacuum. *Appl. Surf. Sci.* **414**, 107–113 (2017)
32. Ni, X., Jin, F., Shen, L., et al.: Carbon fiber/resin composites treated by plasma. *Acta Mater. Compos. Sin.* **32**(3), 721–727 (2015)
33. Blank, W.J., He, Z.A., Picci, M.: Catalysis of the epoxy-carboxyl reaction. *J. Coatings Technol.* **74**(926), 33–41 (2002)
34. Zaldivar, R.J., Nokes, J., Steckel, G.L., et al.: The effect of atmospheric plasma treatment on the chemistry, morphology and resultant bonding behavior of a pan-based carbon fiber-reinforced epoxy composite. *J. Compos. Mater.* **44**(2), 137–156 (2010)
35. Zaldivar, R.J., Kim, H.I., Steckel, G.L., et al.: Surface preparation for adhesive bonding of polycyanurate-based fiber-reinforced composites using atmospheric plasma treatment. *J. Appl. Polym. Sci.* **120**(2), 921–931 (2011)
36. Schäfer, J., Hofmann, T., Holtmannspötter, J., et al.: Atmospheric-pressure plasma treatment of polyamide 6 composites for bonding with polyurethane. *J. Adhes. Sci. Technol.* **29**(17), 1807–1819 (2015)